Heat Conduction and Self-Capacitance from a Cylinder Into an Infinite Uniform Medium

Aubrey G. Jaffer
e-mail: agj@alum.mit.edu

Abstract

This investigation derives formulas to predict the total steady-state heat conduction from an isothermal cylindrical surface in an infinite uniform medium and the self-capacitance of closed and open cylinders.

The conduction formula was tested with 31 natural convection measurements from cylinders having length-to-diameter ratios between 1.48 and 12500 in data-sets from three peer-reviewed studies, yielding (data-set) root-mean-squared relative error values between 1.0% and 4.7%.

The cylinder self-capacitance formulas will be tested with single-ended capacitance measurements of metallic cylinders and disks, each elevated 3.41 m above the ground of an open field.

This research did not receive any specific grant from funding agencies in the public, commercial, or not-for-profit sectors.

Table of Contents

1. Introduction

While exact heat conduction formulas are known for many shapes in an infinite uniform medium, exact formulas for a cylinder in an infinite uniform medium are conspicuously absent from many heat conduction textbooks.

Governed by the same partial differential equations, a related problem is the (electrical) self-capacitance of a cylinder, which was addressed as early as 1877 by James Clerk Maxwell [1].

Modern capacitance investigators overconfidence in numerical simulations has allowed a pervasive faulty assumption about disks to result in a 10% discrepancy when computing their self-capacitance. The heat conduction formula for a double-sided disk is different from a single-sided disk in a semi-infinite space.

There are three cylinder configurations of interest:

- Heat conduction from an isothermal cylinder with adiabatic end faces into an infinite uniform medium.
- Heat conduction from an isothermal cylinder with (isothermal) flat end faces into an infinite uniform medium. Note that this configuration includes disks.

  This configuration is the same as self-capacitance of a conductive "closed cylinder".
- The self-capacitance of an "open cylinder" involving both interior and exterior surfaces.

This investigation does not address local conduction from the cylinder surface or fields within the medium.

1.1 Shape Factors.

The solutions to steady-state heat conduction problems between two isothermal surfaces are customarily expressed using the shape factor S such that heat transfer rate $Q \equiv S\,k\,\Delta T$, where k is the thermal conductivity (with units $\mathrm{W}/(\mathrm{m}\cdot\mathrm{K})$) of the medium between these surfaces and ΔT is the temperature difference between the isothermal surfaces.

For some infinite uniform medium configurations Incropera, DeWitt, Bergman, and Lavine [2] also uses a dimensionless shape factor q^*_{SS} based on surface area A such that:

$$Q = q^*_{SS}\, k\, \Delta T \sqrt{4\,\pi\, A} \qquad S = q^*_{SS} \sqrt{4\,\pi\, A} \tag{1}$$

1.2 **Self-Capacitance.** Self-capacitance is the ability of an object to store electric charge within an infinitely large container at the reference potential (ground).

For self-capacitance in infinite mediums, the $k\,\Delta T$ term is replaced by ε, the permittivity of the uniform medium with units F/m.

The ordinates in the present work capacitance graphs are dimensionless (normalized) self-capacitance $2\,C/[\varepsilon\, D]$.

1.3 **Nusselt Number.** In fluid mechanics, the convective heat transfer rate is represented by the dimensionless average Nusselt number ($\overline{Nu} \equiv \overline{h}\, L_c/k$), where L_c is the characteristic length of the system, A is the area of the surface and $\overline{h} = Q/[A\,\Delta T]$ is the average convective surface conductance, with units $\mathrm{W}/(\mathrm{m}^2 \cdot \mathrm{K})$.

$\overline{Nu}$ and S are simply related:

$$\overline{Nu} \equiv S\, \frac{L_c}{A} \qquad S \equiv \overline{Nu}\, \frac{A}{L_c} \tag{2}$$

The characteristic length L_c is the length scale of a physical system. The characteristic length of a circular cylinder is its diameter D. Generalizing to convex cylinders is the hydraulic diameter, which is 4 times the area-to-perimeter ratio of the cylinder's perpendicular cross-section. Note that the diameter and hydraulic diameter are identical for a circular cylinder.

The relation between $\overline{Nu}$ and q^*_{SS} is slightly more complicated; dimensionless q^*_{SS} uses $\sqrt{A/[4\,\pi]}$ as its characteristic length. Formula (3) swaps $\sqrt{A/[4\,\pi]}$ and L_c:

$$\overline{Nu} \equiv q^*_{SS}\, L_c \sqrt{\frac{4\,\pi}{A}} \qquad q^*_{SS} \equiv \frac{\overline{Nu}}{L_c} \sqrt{\frac{A}{4\,\pi}} \tag{3}$$

2. Data-Sets and Evaluation

Heat transfer measurements were captured from graphs in the cited works by measuring the distance from each point to its graph's axes, then scaling to the graph's units using the "Engauge" software (version 12.1).

Nakai Seiichi and Okazaki Takuro [3] measured natural convection heat transfer from long, thin horizontal wires with $10 \times 10^3 < L/D < 12.5 \times 10^3$ at $Ra < 2 \times 10^{-5}$.

Goldstein, Khan, and Srinivasan [4] measured natural convection mass transfer from three cylinders.

Heo and Chung [5] measured natural convection mass transfer from five cylinders with $3.7 < L/D \leq 13$ at inclinations $0° \leq \vartheta \leq 90°$. Only the four level cylinder measurements ($\vartheta = 0$) are used in the present work.

The results of numerical capacitance simulations were taken from a table in Butler [6] citing Butler in Skwirzynski [7]. The results of numerical integrations were taken from a table in Smythe [8]. Both of these datasets do not reflect actual measurements, only calculations.

Table 1 Cylinder natural convection data-sets

Source	Pr or Sc	L/D	ϑ	$Ra/L^3 \geq$	$Ra/L^3 \leq$	$\pm$	#
Nakai & Okazaki [3]	$Pr = 0.72$	10000–12500	0°	2.5×10^{-7}	1.5×10^{-5}		23
Heo & Chung [5]	$Sc = 2094$	7.4	0°–90°	1.7×10^{14}	1.7×10^{14}	0.9%	13
Heo & Chung [5]	$Sc = 2094$	3.7	0°–90°	1.7×10^{14}	1.7×10^{14}	0.9%	13
Heo & Chung [5]	$Sc = 2094$	13	0°–90°	1.7×10^{14}	1.7×10^{14}	0.9%	9
Heo & Chung [5]	$Sc = 2094$	6.7	0°–90°	1.7×10^{14}	1.7×10^{14}	0.9%	9
Goldstein et al. [4]	$Sc = 2300$	0.63–2.34	0°	3.2×10^{13}	1.6×10^{14}		4

These data files, used for generating the present work graphs and tables, along with digitization details and estimated digitization inaccuracies are available at

`https://people.csail.mit.edu/jaffer/convect/NCHTIC-data.zip`

.

2.1 **RMS Relative Error.** Root-mean-squared (RMS) relative error (RMSRE) provides an objective, quantitative evaluation of theory versus experimental data. It gauges the fit of measurements $g(Ra_j)$ to function $f(Ra_j)$, giving each of the n samples equal weight in Formula (4). Along with presenting RMSRE, charts in the present work split RMSRE into the bias and scatter components defined in Formula (5). The root-sum-squared of bias and scatter is RMSRE.

$$\text{RMSRE} = \sqrt{\frac{1}{n}\sum_{j=1}^{n}\left|\frac{g(Ra_j)}{f(Ra_j)} - 1\right|^2} \tag{4}$$

$$\text{bias} = \frac{1}{n}\sum_{j=1}^{n}\left\{\frac{g(Ra_j)}{f(Ra_j)} - 1\right\} \qquad \text{scatter} = \sqrt{\frac{1}{n}\sum_{j=1}^{n}\left|\frac{g(Ra_j)}{f(Ra_j)} - 1 - \text{bias}\right|^2} \tag{5}$$

3. Prior Work

3.1 **Disk Faces.** Incropera et al. [2] gives a dimensionless shape factor $q^*_{SS} = \sqrt{8}/\pi \approx 0.900$ for both faces of a diameter $L_c = D$ disk in an infinite uniform medium. Using Formulas (1) and (3):

$$A = \frac{\pi D^2}{2} \qquad S = q^*_{SS}\sqrt{4\pi A} = \sqrt{2}\,\pi D \approx 4.443\,D \qquad Nu^\circ_0 = S\frac{D}{A} = \sqrt{8} \approx 2.828 \tag{6}$$

For one face of a diameter D disk into a semi-infinite space Incropera et al. [2] gives $S = 2D$. Thus:

$$A = \frac{\pi D^2}{4} \qquad \frac{D}{A} = \frac{4}{\pi D} \qquad Nu_0 = S\frac{D}{A} = 8/\pi \approx 2.546 \tag{7}$$

- Although the double-sided disk is symmetrical in its plane, the double-sided and single-sided disks have different shape factors and different Nu_0 values!

This is because the flux from the edge of the disk conveys heat from both sides of the double-sided disk, while it conveys heat from only one side of the single-sided disk. The ratio is not 2:1 because the flux from the center of each disk face has negligible interaction with the other side.

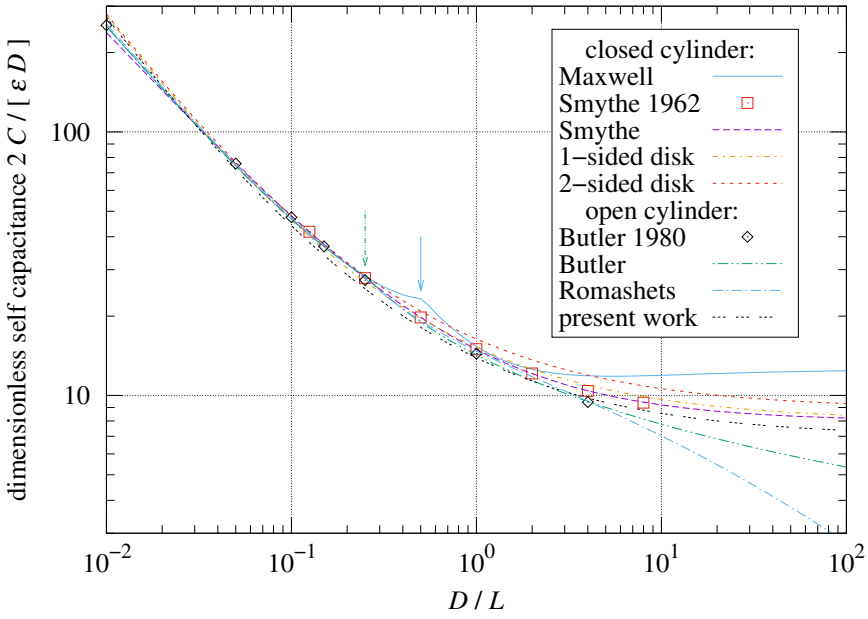

Figure 1 Self-capacitance of cylinder

3.2 **Closed Cylinder.** Maxwell [1] produced a workable approximation of the self-capacitance of the closed cylinder in 1877. This seems to have been forgotten, possibly because of a typographical error (+ instead of −) in its last equation. Corrected and converted to modern units:

$$4\,\pi\,\varepsilon\,\frac{L/2}{\log(4\,L/D)-1} \qquad \frac{D}{L}<\frac{1}{2} \tag{8}$$

$$4\,\pi\,\varepsilon\,\left[\frac{D}{2}-\frac{L}{2\,\pi}\,\log\left(\frac{D}{2\,L}\right)\right] \qquad \frac{D}{L}>\frac{1}{2} \tag{9}$$

The combination of these formulas is shown in Figure 1; the transition between them is marked by an arrow at $D/L = 1/2$.

Smythe [8] gives this formula for self-capacitance of the closed cylinder:

$$\varepsilon\,\frac{D}{2}\,\left[8+6.95\,\left[\frac{L}{D}\right]^{0.76}\right] \qquad \frac{1}{4}<\frac{D}{L}<16 \tag{10}$$

3.3 **Open Cylinder.** Butler [6] investigating the self-capacitance of the open cylinder used Formula (8) (from Maxwell) for long cylinders and Formula (11) for short ones. The transition between them is marked by an arrow at $D/L = 1/4$ in Figure 1.

$$2\,\pi^2\,\varepsilon\,\frac{D}{\log(16\,D/L)} \qquad \frac{D}{L}>\frac{1}{4} \tag{11}$$

Romashets, Vandas, and Sen [9] give a complicated formula for the self-capacitance of an open cylinder. It has been split into pieces and variable names made consistent with the present work for clarity:

$$C=\frac{4\,\pi^2\,\varepsilon\,L}{f+g} \qquad f=\frac{0.0205\,\{1+\tanh\left(8.1-3\,\zeta\right)\}}{\{15.3554\times10^{-6}\,|\,\zeta-6.5\,|^{4.2}+0.009\}^{1.3}} \tag{12}$$

$$g=3.05607\,\{z-0.955856\}\,\{\tanh\left(3\,\{\zeta-2.7\}\right)+1\} \qquad \zeta=\ln\left(\frac{4\,L}{D}\right) \tag{13}$$

4. Development

4.1 **Sphere.** Consider an isothermal diameter D sphere centered within a diameter $\sigma\, D$ envelope sphere filled with a stationary, uniform medium. Because of the radial symmetry, the heat flux gradients flow perpendicularly to the surfaces of both spheres. From Lienhard and Lienhard [10] $\lim_{\sigma\to\infty} S = 2\,\pi\, D$. Hence $\lim_{\sigma\to\infty} Nu_0 = 2$.

The sphere Nu_0 is smaller than the disk Nu_0° because Nusselt numbers are normalized per area, and the disk has half of the sphere area. However, $Nu_0^\circ \neq 2\, Nu_0$ because the flux is constricted by that smaller area near the disk surface.

4.2 **Capsule.** Consider an isothermal capsule composed of a length L diameter D cylinder with diameter D hemispherical end caps aligned and centered within a length L diameter $\sigma\, D$ envelope capsule filled with a stationary, uniform medium.

When $L = 0$, the capsule is a sphere and $\lim_{\sigma\to\infty} Nu_0 = 2$. If the conduction from the cylinder ($L > 0$) were radial, then flux gradients would look something like Figure 2. While the flux gradients from the hemispheres spread with distance, the flux gradients from cylinder do not; they cannot be as large as the hemispherical gradients.

- Thus, the net conduction from a cylinder is not purely radial.

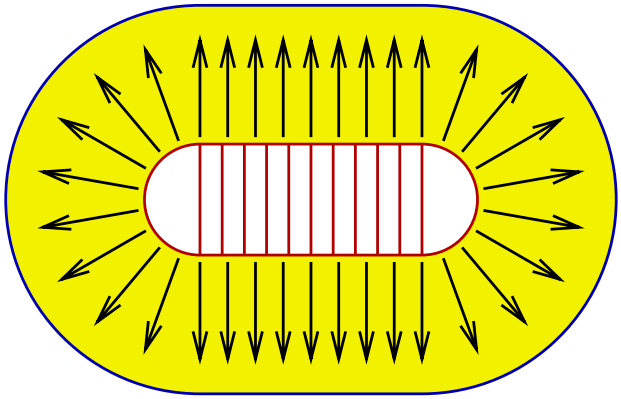

Figure 2 Capsule cross-section with purely radial conduction from cylinder

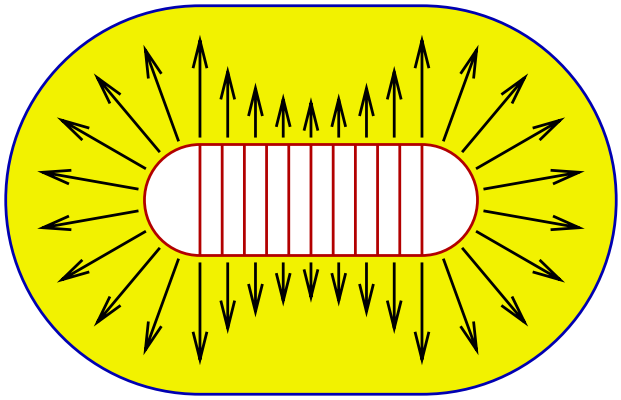

Figure 3 Capsule cross-section with broad conduction from cylinder

Figure 3 is a more plausible rendering of this cross-section. The gradients shown are at the capsule surface; at other points in the medium the gradients will not be perpendicular to the capsule surface.

4.3 **Cylinder With Adiabatic End Faces.** Consider an isothermal length L diameter D cylinder with adiabatic (thermally non-conductive) end faces centered within a length L diameter $\sigma\, D$ envelope capsule filled with a stationary, uniform medium. Without heat flowing from the cylinder's end faces, the cylinder's

radial heat flux lines will curve toward the cylinder axis. Following curved paths, those flux lines must be longer than straight paths, manifesting as reduced conduction and Nu_0.

Without heat flowing from the adiabatic end faces, they cast conical shadows of reduced flux. As σ increases, the cylinder length L becomes less significant than the angular width of the conical flux shadows.

Table 2 Geometric dual comparison

Aspect	Disk	Cylinder
surface	2 flat coplanar surfaces (both disk sides)	1 non-planar surface (exterior only)
border	1 round border coplanar with surfaces	2 flat borders perpendicular to the surface

The cylinder is a geometric dual of the double-sided disk. Table 2 compares their surfaces and borders. The symmetries of Table 2 suggest that $Nu_0^=$ and Nu_0° may be related. With characteristic length D for both, this investigation proposes:

$$\lim_{\sigma\to\infty} Nu_0^= = \frac{1}{Nu_0^\circ} = \frac{1}{\sqrt{8}} \approx 0.3536 \qquad S = Nu_0^= \frac{A}{D} = \frac{\pi}{\sqrt{8}} L \approx 1.111\, L \tag{14}$$

- $Nu_0^=$ does not depend on L (or D). If Formula (14) is correct, then it is valid for all length cylinders.
- However, $\lim_{L\to\infty} S$ does not exist.

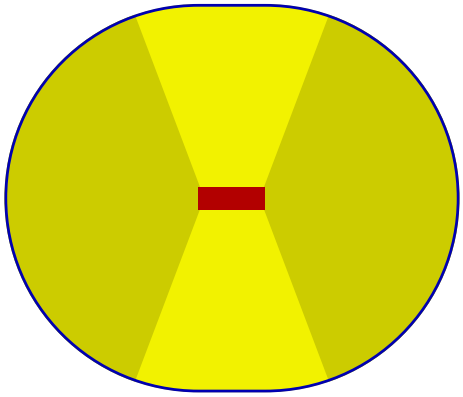

Figure 4 Schematic of flux shadows from adiabatic end faces

If the shadow boundaries were abrupt, the angle subtended by each cone would be 138.6°; hypothetical abrupt shadows from a horizontal cylinder (red) are darkened in Figure 4.

4.4 **Combining Transfer Processes.** Formula (15) is an unnamed form for combining functions which appears frequently in heat or mass transfer formulas:

$$F^p = F_1^p + F_2^p \tag{15}$$

Churchill and Usagi [11] stated that such formulas are "remarkably successful in correlating rates of transfer for processes which vary uniformly between these limiting cases." Conduction and convection transfer heat (or solute) between the cylinder and the medium.

When $F_1 \geq 0$ and $F_2 \geq 0$, taking the pth root of both sides of Equation (15) yields a vector-space functional form known as the ℓ^p-norm, which is notated $\|F_1\ ,\ F_2\|_p$:

$$\|F_1\ ,\ F_2\|_p \equiv [\ |F_1|^p + |F_2|^p]^{1/p} \tag{16}$$

A vector-space norm with $p \geq 1$ obeys the triangle inequality: $\|F_1, F_2\|_p \leq |F_1| + |F_2|$.

When $p > 1$, the processes modeled by F_1 and F_2 compete and $\|F_1, F_2\|_p \geq \max(|F_1|, |F_2|)$; the most competitive case is $\|F_1, F_2\|_{+\infty} \equiv \max(|F_1|, |F_2|)$.

The ℓ^1-norm (addition) models independent processes; $\|F_1, F_2\|_1 \equiv |F_1| + |F_2|$.

When $0 < p < 1$, the processes cooperate and $\|F_1, F_2\|_p \geq |F_1| + |F_2|$. Cooperation between conduction and flow-induced heat transfer can occur in natural convection systems.

4.5 **Cylinder With Isothermal End Faces.** Consider a cylinder whose flat end faces are at the same temperature as the cylinder surface in an infinite uniform medium. When $L = 0$, then $Nu_0^\bullet = \sqrt{8}$, the same as a disk with characteristic length D.

Because the areas of the cylinder and disk may be different, their Nusselt numbers cannot be directly combined, although their shape factors can.

As seen in Figure 4, some heat from a cylinder with isobaric faces flows into spaces through which disk heat flows. When the faces are present, the cylinder heat bends less than if absent. The cylinder and disk faces cooperate as the ℓ^p-norm with $p = 1/\sqrt[4]{8} \approx 0.595$:

$$\frac{Q}{k\,\Delta T} = \left\| \frac{Nu_0^= \pi\, D\, L}{D}, \frac{Nu_0^\circ \pi\, D^2}{2\, D} \right\|_p = \left\| \frac{\pi\, L}{\sqrt{8}}, \frac{\sqrt{8}\,\pi\, D}{2} \right\|_p = S \tag{17}$$

$$Nu_0^\bullet = S\,\frac{D}{A} = \frac{\left\| L/\sqrt{8}, \sqrt{8}\, D/2 \right\|_p}{L + D/2} \tag{18}$$

The limits which exist for S are:

$$\lim_{D\to 0} S = \frac{\pi\, L}{\sqrt{8}} \qquad \lim_{L\to 0} S = \frac{\sqrt{8}\,\pi\, D}{2} \tag{19}$$

With $L > 0$ and $D > 0$, the $Nu_0^\bullet$ limits to 0 and ∞ exist:

$$\lim_{D\to 0} Nu_0^\bullet = \lim_{L\to\infty} Nu_0^\bullet = \frac{1}{\sqrt{8}} \qquad \lim_{L\to 0} Nu_0^\bullet = \lim_{D\to\infty} Nu_0^\bullet = \sqrt{8} \tag{20}$$

4.6 **Open Cylinder.** The long open cylinder has twice the surface area of the long closed cylinder, but very little of the inside flux escapes. Very short open cylinders are treated as an L diameter wire which is $\pi\, D$ long. Because Nu_0 is normalized for area, Nu_0 is halved. As with the closed cylinder, $p = 1/\sqrt[4]{8} \approx 0.595$:

$$\frac{C}{\pi\,\varepsilon} = \left\| \frac{L}{\sqrt{8}}, \frac{\pi\, D}{\sqrt{8}} \right\|_p = S \qquad Nu_0 = \frac{1}{2\, L} \left\| \frac{L}{\sqrt{8}}, \frac{\pi\, D}{\sqrt{8}} \right\|_p = \frac{1}{2} \left\| \frac{1}{\sqrt{8}}, \frac{\pi\, D}{\sqrt{8}\, L} \right\|_p \tag{21}$$

The limits which exist for S are:

$$\lim_{D\to 0} S = \frac{\pi\, L}{\sqrt{8}} \qquad \lim_{L\to 0} S = \frac{\pi\, D}{\sqrt{8}} \tag{22}$$

With $D > 0$, the Nu_0 limits are:

$$\lim_{D\to 0} Nu_0 = \lim_{L\to\infty} Nu_0 = \frac{1}{\sqrt{8}} \tag{23}$$

5. Natural Convection

Natural convection depends on static fluid conduction. From Jaffer [12] comes Formula (24) for natural convection from a level cylinder:

$$\overline{Nu} = \left\| \frac{Nu_0^=}{2} \ , \ \sqrt[2+E^\bullet]{\left[\frac{\pi\, Nu_0^=}{6}\right]^{3+E^\bullet} \frac{Ra_D}{\pi\, \Xi_\bullet}} \right\|_{1/3} \qquad \Xi_\bullet = \left\| 1 \ , \ \frac{\sqrt{1/3}}{Pr} \right\|_{\sqrt{1/3}} \tag{24}$$

$$E^\bullet = \frac{5}{6} + \frac{11}{9\,\pi} \approx 1.222 \tag{25}$$

Formula (24) shows that $Nu_0^=$ scales $\overline{Nu}$ throughout its range of Ra_D. Unless Formula (24) has an error exactly matched to Formula (14), an incorrect $Nu_0^=$ will cause incorrect predictions from Formula (24).

End faces are treated separately from the cylinder in natural convection calculations because their heat transfers are governed by different equations. Formula (18) shows that $Nu_0^=$ dominates Nu_0° when $\text{Ł} \gg D$, allowing $Nu_0^=$ to be isolated from end face conduction when $\text{Ł} \gg D$.

Nakai and Okazaki [3] measured natural convection heat transfer from very long, thin horizontal wires with $L/D > 10000$. Relative to Formula (24), their 23 measurements (shown in Figure 5) have 1.0% RMSRE.

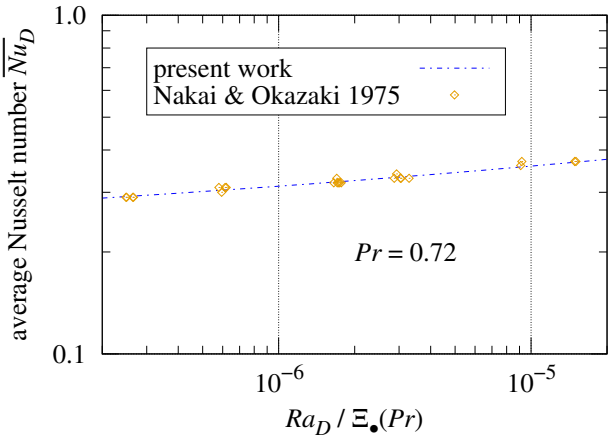

Figure 5 Natural convection from level cylinder in air

The same formulas which govern natural convection heat transfer also govern solute transfer with Sherwood number $\overline{Sh}$ replacing $\overline{Nu}$ and Schmidt number Sc replacing Pr. Solute transfer studies where the cylinder ends do not accept or supply solute correspond to isothermal cylinders with adiabatic end faces, allowing short cylinders to be tested as well.

Goldstein et al. [4] measured copper electroplating onto three cylinders in a $CuSO_4/H_2SO_4$ solution. The cylinders were 78.8 mm in diameter and had lengths 49.9 mm, 116.4 mm, and 184.4 mm. They presented measurements without identifying the cylinder used in each trial. The present analysis treats all as having length, 116.4 mm.

Heo and Chung [5] measured copper electroplating onto a copper cylinder in a $CuSO_4/H_2SO_4$ solution at a variety of inclinations. Only the level cylinder measurements are presented here.

Table 3 Level cylinder measurements versus Formula (24)

Source	Pr or Sc	L/D	ϑ	RMSRE	Bias	Scatter	#
Goldstein et al. [4]	$Sc = 2300$	0.63–2.34	0°	4.7%	−4.4%	1.6%	4
Heo & Chung [5]	$Sc = 2094$	3.73–13.2	0°	1.4%	+0.3%	1.3%	4
Nakai & Okazaki [3]	$Pr = 0.72$	10000–12500	0°	1.0%	−0.1%	1.0%	23

Table 3 and Figure 6 compare Formula (24) with data-sets from Goldstein et al. [4], Heo and Chung [5], and Nakai and Okazaki [3].

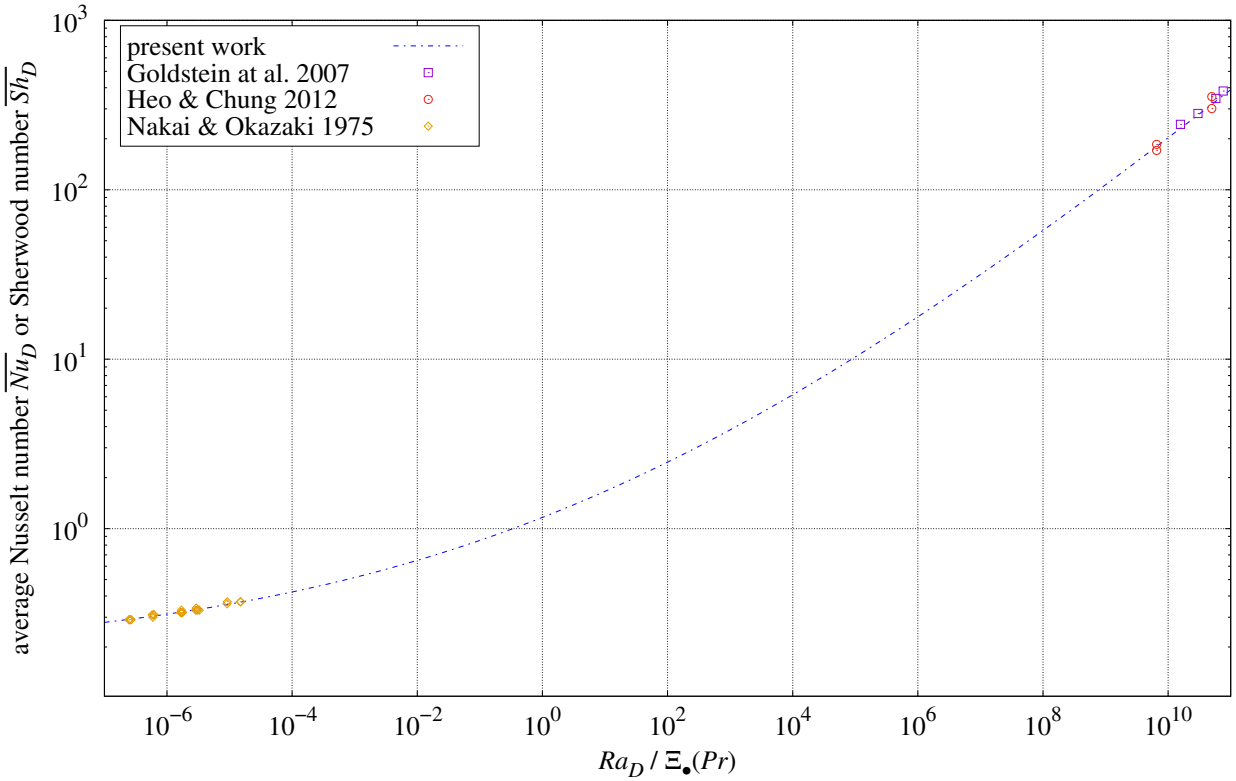

Figure 6 Natural convection from level cylinder

6. Capacitance

This investigation plans to measure the self-capacitance of a 0.3 m circular plate, a 0.35 m wire hoop, a thin 1 m long pipe, and a 0.1 m diameter, 0.4 m long cylinder (closed and open), each atop a 3.41 m pole in an open field. Each object has been sized so its capacitance is expected to be about 12 pF. The 0.254 mm wire connecting the base to the object is 3.41 m long. It has 34 pF of self-capacitance, 1.15 Ω of resistance, and 6.92 μH of inductance. At the pole's base a Colpitts oscillator generates a signal at the resonant frequency of the wire's inductance with its capacitance, about 10.4 MHz. When the test device is connected, its capacitance lowers the resonant frequency to about 8.92 MHz. The test object self-capacitance can thus be inferred from oscillation frequency.

Table 4 Expected device self-capacitance

End Faces	D	L	D/L	Pure	Vertical	Level
closed	0.305.m	3.18.mm	96	12.6.pF	12.9.pF	12.6.pF
closed	0.102.m	0.406.m	0.25	12.8.pF	12.9.pF	13.0.pF
closed	6.35.mm	1.02.m	0.00625	11.9.pF	11.9.pF	11.9.pF
open	0.356.m	3.28.mm	108.53	11.6.pF	11.6.pF	11.6.pF
open	0.102.m	0.406.m	0.25	11.4.pF	11.4.pF	11.6.pF

Lienhard and Lienhard [10] gives the sphere $S = 2\,\pi\,D$; for a sphere whose center is h from an isothermal plane (equivalent to a ground plane):

$$S = 2\,\pi\,D \Big/ \left[1 - \frac{D}{4\,h}\right] \qquad Nu_0 = 2 \Big/ \left[1 - \frac{D}{4\,h}\right]$$

Thus $1 - D/[4\,h]$ is a reciprocal factor for the ground proximity. To generalize this to shapes other than spheres, replace D with the hydraulic diameter of the normal projection of the object onto the ground plane.

Table 4 lists expected self-capacitance of the test objects. The "Pure" column lists expected capacitance of each object in isolation. The "vertical" column lists expected capacitance with the D dimension parallel to the ground plane; The "level" column is with the L dimension parallel to the ground plane.

7. Comparison of Theories

Figure 7 plots Nu_0 versus $0.001 < D/L < 1000$ for each theory. Table 5 lists Nu_0 values at $D/L = 10^4, 10^8, 10^{-4}$, and 10^{-8} for each theory.

The open cylinder theories have lower Nu_0 than the closed cylinder theories because their areas include both the interior and exterior surfaces of the cylinder.

There is general agreement between the theories at $0.03 < D/L < 3$. At $D/L < 0.03$ there is significant divergence. The "1-sided disk" and "2-sided disk" entries approach 0.354, which is the present work adiabatic Nu_0. Similarly, the open cylinder "present work" entries approaches $0.354/2 = 0.177$. The other theories have much smaller Nu_0 values. The Nakai and Okazaki [3] data matches $Nu_0 = 0.354$ within 1% in Table 3.

At large D/L ratios, the closed cylinder becomes a (double-sided) disk with Nu_0 approaching Formula (6) $\sqrt{8} \approx 2.828$. This is the case for the (present work) "2-sided disk". But "Smythe" and "1-sided disk" approach Formula (7) $Nu_0 = 2.546$, which is Nu_0 of a single-sided disk in a semi-infinite medium.

At large D/L ratios, the "Butler" and "Romashets" open cylinder curves are decreasing, but at different rates. The "present work" curve approaches a constant 2.221. The planned self-capacitance measurement of a $D/L \approx 100$ wire hoop should be able to validate one of the curves.

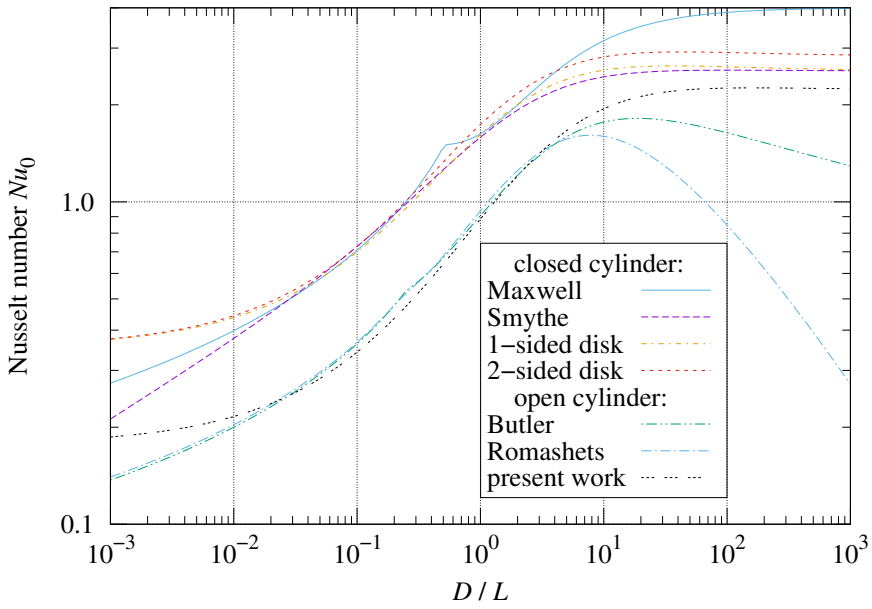

Figure 7 Nu_0 **of cylinder**

Table 5 Nu_0 **asymptotes**

Source	**End Faces**	$L/D = 10^4$	$L/D = 10^8$	$L/D = 10^{-4}$	$L/D = 10^{-8}$
present work	adiabatic	0.354	0.354	0.354	0.354
Maxwell [1]	closed	0.208	0.106	3.998	4.000
Smythe [8]	closed	0.121	0.013	2.548	2.546
1-sided disk	closed	0.359	0.354	2.554	2.547
2-sided disk	closed	0.359	0.354	2.837	2.828
Butler [6]	open	0.104	0.053	1.048	0.593
Romashets et al. [9]	open	0.107	0.055	0.070	0.000
present work	open	0.179	0.177	2.228	2.221

8. Discussion

Conduction Nusselt numbers (Nu_0) hold an advantage over S shape factors in predicting conduction from an isothermal 3-dimensional object in an infinite uniform medium because they are scaled for area; Nu_0 is bounded as the object dimensions increase.

Prior work difficulty finding a solution to cylinder conduction arose from a couple of factors:

- "Infinite-length" analysis of the cylinder sliced perpendicular to its axis.
- Use of shape-factor S instead of Nu_0 obscured the simple relationship between $Nu_0^{=}$ and $Nu_0^{\bullet}$, and the fact that their asymptotic D and L limits existed.

8.1 **Testing cylinder with conductive end caps.** Natural convection is unsuitable for testing cylinders with conductive end caps because the natural convection from the ends has different dependencies on D and Ra than the cylinder.

Measuring electrical capacitance from a cylinder should be employed to test Formula (18).

9. References

[1] James Clerk Maxwell. On the electrical capacity of a long narrow cylinder, and of a disk of sensible thickness. *Proceedings of the London Mathematical Society*, s1-9:94–102, November 1877, doi:10.1112/plms/s1-9.1.94.

[2] F.P. Incropera, D.P. DeWitt, T.L. Bergman, and A.S. Lavine. *Fundamentals of Heat and Mass Transfer*. Wiley, Hoboken, NJ, USA, 2007.

[3] Nakai Seiichi and Okazaki Takuro. Heat transfer from a horizontal circular wire at small reynolds and grashof numbers. *International Journal of Heat and Mass Transfer*, 18(3):387–396, 1975, doi:10.1016/0017-9310(75)90028-9.

[4] R.J. Goldstein, V. Khan, and V. Srinivasan. Mass transfer from inclined cylinders at moderate rayleigh number including the effects of end face boundary conditions. *Experimental Thermal and Fluid Science*, 31(7):741–750, 2007, doi:10.1016/j.expthermflusci.2006.08.001.

[5] Jeong-Hwan Heo and Bum-Jin Chung. Natural convection heat transfer on the outer surface of inclined cylinders. *Chemical Engineering Science*, 73:366–372, 2012, doi:10.1016/j.ces.2012.02.012.

[6] Chalmers M. Butler. Capacitance of a finite-length conducting cylindrical tube. *Journal of Applied Physics*, 51(11):5607–5609, 11 1980, doi:10.1063/1.327575.

[7] J.K. Skwirzynski, editor. *Theoretical Methods for Determining the Interaction of Electromagnetic Waves with Structures*. NATO Science Series E. Springer Dordrecht, 2012.

[8] W. R. Smythe. Charged right circular cylinder. *Journal of Applied Physics*, 33(10):2966–2967, 10 1962, doi:10.1063/1.1728544.

[9] E. Romashets, M. Vandas, and C. Sen. Capacitance of a conducting hollow cylindrical shell in a closed form. *Journal of Electrostatics*, 126:103866, 2023, doi:10.1016/j.elstat.2023.103866.

[10] J. H. Lienhard, V and J. H. Lienhard, IV. *A Heat Transfer Textbook*. Phlogiston Press, Cambridge, MA, 6th edition, April 2024. Version 6.00.

[11] S. W. Churchill and R. Usagi. A general expression for the correlation of rates of transfer and other phenomena. *AIChE Journal*, 18(6):1121–1128, 1972, doi:10.1002/aic.690180606.

[12] Aubrey Jaffer. Natural convection heat transfer from an inclined cylinder. *Thermo*, 6(1), 2026, doi:10.3390/thermo6010019.